Nutrient distribution and metabolism in the intervertebral disc in the unloaded state: a parametric study

Carole Magnier, Olivier Boiron, Sylvie Wendling-Mansuy, Patrick Chabrand, Valérie Deplano

Nutrient distribution and metabolism in the intervertebral disc in the unloaded state: A parametric study

Carole Magnier [a,*], Olivier Boiron [b], Sylvie Wendling-Mansuy [a], Patrick Chabrand [a], Valérie Deplano [b]

[a] *Institute of Movement Sciences CNRS UMR 6233, Interdisciplinary Group of Osteoarticular Biomechanics, Aix-Marseilles University, Marseilles, France*
[b] *IRPHE CNRS UMR 6594, Cardiovascular Biomechanics Group, Aix-Marseilles University and Ecole Centrale of Marseilles, France*

A 2-D finite element model for the intervertebral disc in which quadriphasic theory is coupled to the transport of solutes involved in cellular nutrition was developed for investigating the main factors contributing to disc degeneration. Degeneration is generally considered to result from chronic disc cell nutrition insufficiency, which prevents the cells from renewing the extracellular matrix and thus leads to the loss of proteoglycans. Hence, the osmotic power of the disc is decreased, causing osmomechanical impairments. Cellular metabolism depends strongly on the oxygen, lactate and glucose concentrations and on pH in the disc. To study the diffusion of these solutes in a mechanically or osmotically loaded disc, the osmomechanical and diffusive effects have to be coupled. The intervertebral disc is modeled here using a plane strain formulation at the equilibrium state under physiological conditions after a long rest period (called unloaded state). The correlations between solute distribution and various properties of healthy and degenerated discs are investigated. The numerical simulation shows that solute distribution in the disc depends very little on the elastic modulus or the proteoglycan concentration but greatly on the porosity, diffusion coefficient and endplate diffusion area. This coupled model therefore opens new perspectives for investigating intervertebral disc degeneration mechanisms.

1. Introduction

Back pain is a major public health problem in Western countries. This complaint is often due to the degeneration of one or several intervertebral discs (IVDs). The degeneration process involves structural and constitutional changes (Antoniou et al., 1996; Thompson et al., 1990), making the disc unable to perform its mechanical role efficiently: healthy discs absorb and redistribute external loads over the spine via the osmotic pressure exerted by proteoglycans, by evacuating during activity periods part of their water content, which is reabsorbed during rest periods (Boos et al., 1993). Degenerated discs contain fewer proteoglycans than healthy ones (Antoniou et al., 1996) and therefore exert weaker osmotic pressures (Urban and McMullin, 1985), thus limiting the fluid exchanges. Degeneration is generally assumed to result from chronic disc cell nutritional insufficiency (Brodin, 1955). These cells, which are responsible for extracellular matrix maintenance, consume the glucose and oxygen they require to live and function principally via a process of anaerobic glycolysis, the main waste product of which is lactate. Their metabolism depends strongly on the concentrations of these solutes and on the pH level in the disc (Bibby and Urban, 2004).

The highly complex degeneration mechanisms involved were previously investigated using numerical models of two kinds: osmomechanical models describing the loaded disc's behavior and nutrient diffusion models describing the nutrient transport and metabolism in a fixed disc. Biphasic swelling models considered the disc to consist of a solid phase representing its extracellular matrix, to which a fixed charge density (FCD) representing proteoglycans is bound, and a fluid phase, and were able to predict disc equilibrium (Schroeder et al., 2006). Tri/quadriphasic models, in which two ionic phases equilibrating the electric charges are added, can predict the transient behavior of the disc (Huyghe and Janssen, 1997). The mechanical and osmotic properties of the disc subjected to several loads were determined using this approach (Frijns et al., 1997; Huyghe et al., 2003). Diffusion models governed by Fick's law were developed for studying the relationships between cellular metabolism and solute concentrations in the disc. Sélard et al. (2003) were the first to study glucose, oxygen and lactate transport in an axisymmetric disc via the metabolic reaction rates depending nonlinearly on the corresponding solute concentration. More complex metabolic reaction rates were then modeled by taking the coupling between glucose consumption and lactate

* Corresponding author at: Groupe Interdisciplinaire de Biomécanique Ostéoarticulaire (GIBO), Institut des Sciences du Mouvement CNRS UMR 6233, Université de la Méditerranée, 163, avenue de Luminy, Case 910, F-13288 Marseille Cedex 09, France. Tel.: +33 4 91 26 60 30; fax: +33 4 91 41 16 91.
E-mail address: carole.magnier@etumel.univmed.fr (C. Magnier).

production (Soukane et al., 2005) and the dependence of these rates on the oxygen and lactate concentrations and on the pH levels (Soukane et al., 2007) into account. The latter authors computed the effects on solute spatial distribution of parameters reflecting disc degeneration: the variation of disc thickness, exchange area with blood flux, cellular reaction rates and diffusivity.

Huang and Gu (2008) were the first to characterize the IVD behavior using a quadriphasic model including nutrient transport and cellular metabolism. This coupling is necessary to determine how osmomechanical properties and load affect the spatial distribution of nutrients and thus the cellular metabolism. In their model, the solid matrix behavior was assumed to be tension–compression nonlinear and oxygen and lactate were transported by convection and diffusion. However, the glucose concentration, which is fundamental for cell viability (Bibby and Urban, 2004), was not considered. They examined the effect of static and dynamic compression on oxygen concentration and pH. The present parametric study also combines both kinds of models but a linear behavior for the solid phase is assumed, and oxygen, lactate and glucose are transported by diffusion. The correlations between nutrient distribution and disc properties in healthy and degenerated cases are investigated.

2. Model and methods

2.1. Geometry

The IVD was modeled in the sagittal plane, using a 2-D plane strain formulation, to show the behavioral asymmetry between the anterior and posterior parts of the disc. Assuming the existence of symmetry about the mid-horizontal plane, the problem was reduced to the upper half-disc. The geometry and dimensions, which are largely inspired from X-ray measurements of a L3/L4 IVD (Lavaste et al., 1992), are described in Fig. 1 for the healthy disc with uniform height. The half-thickness of the nucleus and annulus was reduced to 4.5 mm for the degenerated disc. An intervertebral angle of 8° (Kimura et al., 2001) was considered for the healthy disc with non-uniform height.

2.2. Quadriphasic model for the IVD including nutrient transport

In the quadriphasic model (Huyghe and Janssen, 1997), the IVD was taken to be a multiphasic material consisting of a solid phase (s) formed mostly by collagen fibers and proteoglycans, a fluid phase (f), an anionic phase ($-$) and a cationic phase ($+$). The solid phase is porous, intrinsically incompressible and saturated with saline water (ionic and fluid phases). In order to couple the nutrient diffusion process to the osmomechanical behavior of the disc, oxygen (O_2), lactate (lact) and glucose (gluc) were included in the quadriphasic model, forming three additional uncharged phases. The triplet oxygen, lactate and glucose will henceforth be called nutrients (ω).

Space is divided into two domains: the IVD (Ω) is separated from the outside ($\overline{\Omega}$) by a membrane that is impermeable to proteoglycans but permeable to salts and water. Ω is divided into several subdomains corresponding to its characteristic structural zones: the nucleus pulposus, vertebral endplate, and anterior/posterior inner/outer annulus fibrosus. Unless stated otherwise, the following equations are all valid in Ω.

To study disc equilibrium under physiological conditions after a long rest period, a stationary problem is therefore solved.

2.2.1. Conservation of mass

Let ϕ denote the fluid volume fraction. The system is saturated and the ionic and nutrient volume fractions are negligible in comparison with the solid and fluid volume fractions. The solid volume fraction is therefore equivalent to $1-\phi$. It is assumed that no chemical reactions take place in the medium. Conservation of mass by each component requires the following:

$$div((1-\phi)\rho_T^s \overrightarrow{v^s}) = 0 \tag{1}$$

$$div(\phi\rho_T^f \overrightarrow{v^f}) = 0 \tag{2}$$

$$div(\phi M^\alpha c^\alpha \overrightarrow{v^\alpha}) = 0 \quad (\alpha = +, -) \tag{3}$$

$$div(\phi M^\omega c^\omega \overrightarrow{v^\omega}) = M^\omega R'_\omega \tag{4}$$

where ${\rho_T}^s$ and ${\rho_T}^f$ are the true solid and water density, respectively, $\overrightarrow{v^\beta}$ ($\beta = s, f, +, -, \omega$) is the velocity of the β component, M^δ ($\delta = +, -, \omega$) is the molecular weight of the solute δ, c^δ is its molar concentration and R'_ω is the metabolic reaction rate of the nutrient ω.

Assuming the occurrence of small perturbations, the total change in the volume can be expressed in terms of the strain tensor $\overline{\overline{\varepsilon}}$ as

$$\frac{V}{V_0} = 1 + tr(\overline{\overline{\varepsilon}}) \tag{5}$$

Giving

$$\phi = \phi_0 + (1-\phi_0)tr(\overline{\overline{\varepsilon}}) \tag{6}$$

2.2.2. Electroneutrality condition

Let c^{fc} denote the FCD, which is related to the proteoglycan concentration (Loret and Simões, 2004), and z the ionic valence. The electroneutrality condition is

$$z^+c^+ + z^-c^- - c^{fc} = 0 \tag{7}$$

The main ions present in the disc are Na^+ and Cl^-. Disc ions are therefore assumed to be monovalent and Eq. (7) can be rewritten as

$$\text{In } \Omega,\ c^+ = c^- + c^{fc} \tag{8}$$

$$\text{In } \overline{\Omega},\ \overline{c^+} = \overline{c^-} = \overline{c} \tag{9}$$

It is assumed that proteoglycans undergo no quantitative changes:

$$c^{fc}V^f = c_0^{fc}V_0^f \Rightarrow c^{fc} = c_0^{fc}\left(1 - \frac{tr\overline{\overline{\varepsilon}}}{\phi_0}\right) \tag{10}$$

2.2.3. Equilibrium equation and second law of thermodynamics

Magnetic and gravitational effects are neglected. The gradients of the (electro)chemical potentials μ^α ($\alpha = f, +, -, \omega$) are the driving forces, balanced by the frictional forces between phases.

The mechanical equilibrium is given by

$$\overrightarrow{div}(\overline{\overline{\sigma}}) = \vec{0} \tag{11}$$

where $\overline{\overline{\sigma}}$ is the total stress tensor.

In agreement with the second law of thermodynamics, the following relation is assumed:

$$-\rho^\alpha \vec{\nabla}\mu^\alpha + \sum_\beta \overline{\overline{f_{\alpha\beta}}}(\vec{v}^\beta - \vec{v}^\alpha) = \vec{0}\,(\alpha = f, +, -, \omega; \quad \beta = s, f, +, -, \omega) \tag{12}$$

where $\rho^\alpha = \phi\rho_T{}^\alpha$ if $\alpha = f$ and $\rho^\alpha = \phi M^\alpha c^\alpha$ otherwise.

The frictional coefficients between solid and ions, cations and anions, solid and nutrients, nutrients and ions and between two nutrients are neglected. The remaining coefficients are assumed to be scalar and are related to the diffusion

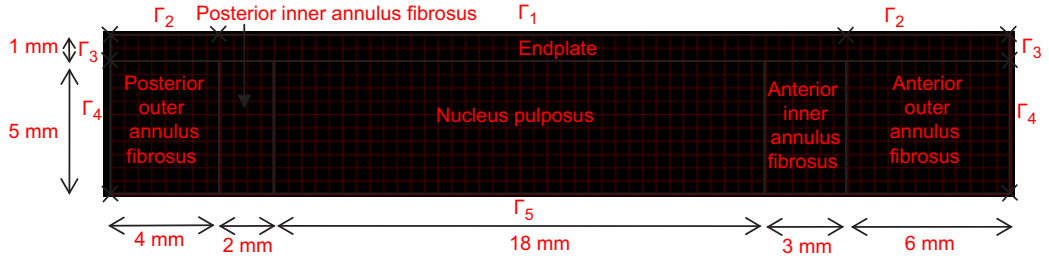

Fig. 1. Initial geometry and mesh of the healthy IVD with uniform height.

coefficients of the solutes in the solution D^δ ($\delta = +, -, \omega$) or to the permeability coefficient k in the relations

$$\frac{k}{\phi^2} = f_{fs}^{-1} \text{ and } D^\delta = RT\phi c^\delta f_{f\delta}^{-1} \tag{13}$$

where R is the universal gas constant and T is the absolute temperature.

Assuming that the convective part of the transport is negligible in comparison with the diffusive part for nutrients (Urban et al., 1982; Katz et al., 1986), Eq. (4) therefore becomes

$$-div(\phi D^\omega \vec{\nabla} c^\omega) = R'_\omega \tag{14}$$

2.2.4. Constitutive equations

The relation between stress, strain and pressure p is written as

$$\overline{\overline{\sigma}} = \overline{\overline{C}} : \overline{\overline{\varepsilon}} - p\overline{\overline{I}} \tag{15}$$

where $\overline{\overline{C}}$ is the stiffness tensor and $\overline{\overline{I}}$ the unit tensor.

The relations between (electro)chemical potentials, pressure, electrical potential ψ and solute concentrations are written as follows:

In Ω,

$$\mu^+ = \mu_0^+ + \frac{RT\ln\left(\gamma^+\frac{c^+}{c_0}\right)}{M^+} + \frac{F\psi}{M^+} \tag{16}$$

$$\mu^- = \mu_0^- + \frac{RT\ln\left(\gamma^-\frac{c^-}{c_0}\right)}{M^-} - \frac{F\psi}{M^-} \tag{17}$$

$$\mu^f = \mu_0^f + \frac{p - RT\Phi(c^+ + c^-)}{\rho_T^f} \tag{18}$$

$$\mu^\omega = \mu_0^\omega + \frac{RT\ln\left(\frac{c^\omega}{c_0}\right)}{M^\omega} \tag{19}$$

In $\overline{\Omega}$, taking $\overline{p} = 0$ and $\overline{\psi} = 0$,

$$\overline{\mu^+} = \mu_0^+ + \frac{RT\ln(\overline{\gamma}^+\overline{c})}{M^+} \tag{20}$$

$$\overline{\mu^-} = \mu_0^- + \frac{RT\ln(\overline{\gamma}^-\overline{c})}{M^-} \tag{21}$$

$$\overline{\mu^f} = \mu_0^f - \frac{2RT\overline{\Phi}\overline{c}}{\rho_T^f} \tag{22}$$

$$\overline{\mu^\omega} = \mu_0^\omega + \frac{RT\ln\overline{c^\omega}}{M^\omega} \tag{23}$$

where F is the Faraday constant, γ^α (respectively $\overline{\gamma}^\alpha$) ($\alpha = +, -$) is the inner (respectively outer) activity coefficient and Φ (respectively $\overline{\Phi}$) the inner (respectively outer) osmotic coefficient.

2.2.5. Metabolic reaction rates

The cellular metabolism laws used in this model were established by Bibby et al. (2005), based on *in vitro* experiments on bovine IVD cells, and previously used in their models by Soukane et al. (2007) and Huang and Gu (2008).

The oxygen consumption rate R_{O_2} (in nmol million cell^{-1} h^{-1}) is written as

$$R_{O_2} = \frac{7.28[O_2](\text{pH} - 4.95)}{1.46 + [O_2] + 4.03(\text{pH} - 4.95)} \tag{24}$$

where $[O_2]$ is the partial oxygen pressure in kPa

The partial pressure can be converted into a molar concentration c^{O_2} as follows:

$$c^{O_2} = s[O_2] \tag{25}$$

where s is the solubility of oxygen in water

The lactate production rate R_{lact} (in nmol million cell^{-1} h^{-1}) is written as

$$R_{lact} = e^{(-2.47+0.93\text{pH}+0.16[O_2]-0.0058[O_2]^2)} \tag{26}$$

Since the glycolic pathway is adopted for the cellular metabolism:

$$R_{gluc} = 0.5\, R_{lact} \tag{27}$$

It is worth noting that $R'_{O_2} = -R_{O_2}$, $R'_{gluc} = -R_{gluc}$ (species consumed) and $R'_{lact} = R_{lact}$ (species produced).

Data obtained by Soukane et al. (2007) are linearized to link pH to c_{lact}.

$$\text{pH} = 7.4 - 0.09\, c_{lact} \tag{28}$$

A system of three diffusive equations coupled by nonlinear relations between species is thus obtained.

2.2.6. Solution of the equations

The system's unknowns are the displacement, three variables derived from (electro)chemical potentials $L^f = \rho_T^f(\mu^f - \overline{\mu}^f)$, $L^+ = M^+(\mu^+ - \overline{\mu}^+)$ and $L^- = M^-(\mu^- - \overline{\mu}^-)$ and the nutrient concentrations.

From Eqs. (8), (9), (16)–(18) and (20)–(22), we obtain

$$c^+ = \frac{c^{fc} + \sqrt{(c^{fc})^2 + 4\frac{\overline{\gamma}^+\overline{\gamma}^-}{\gamma^+\gamma^-}\overline{c}^2 e^{((L^+ + L^-)/RT)}}}{2} \tag{29}$$

$$c^- = \frac{-c^{fc} + \sqrt{(c^{fc})^2 + 4\frac{\overline{\gamma}^+\overline{\gamma}^-}{\gamma^+\gamma^-}\overline{c}^2 e^{((L^+ + L^-)/RT)}}}{2} \tag{30}$$

$$p = L^f + \pi_{Donnan} \text{ with } \pi_{Donnan} = \text{RT}\left(\Phi\sqrt{(c^{fc})^2 + 4\frac{\overline{\gamma}^+\overline{\gamma}^-}{\gamma^+\gamma^-}\overline{c}^2 e^{((L^+ + L^-)/RT)}} - 2\overline{\Phi}\overline{c}\right) \tag{31}$$

$$\psi = \frac{1}{2F}\left(L^+ - L^- - RT\ln\left(\frac{\gamma^+\overline{\gamma}^-}{\overline{\gamma}^+\gamma^-}\frac{c^{fc} + \sqrt{(c^{fc})^2 + 4\frac{\overline{\gamma}^+\overline{\gamma}^-}{\gamma^+\gamma^-}\overline{c}^2 e^{((L^+ + L^-)/RT)}}}{-c^{fc} + \sqrt{(c^{fc})^2 + 4\frac{\overline{\gamma}^+\overline{\gamma}^-}{\gamma^+\gamma^-}\overline{c}^2 e^{((L^+ + L^-)/RT)}}}\right)\right) \tag{32}$$

The coupled equation system is solved by substituting Eqs. (12) and (13) into (2) and (3) and using Eqs. (6), (10), (11), (14), (15) and (24)–(32).

2.3. Boundary and interface conditions

The disc is initially in the stress-free state (i.e. fixed to the adjacent vertebrae, not swollen and bathed in a saturated saline solution) and is brought into the prestressed unloaded state (i.e. fixed to the adjacent vertebrae and free to swell in a physiological saline solution) (Fig. 2).

The displacements are therefore constrained to zero at the endplate, and the outer solution is adjusted from saturated to physiological. At equilibrium, the (electro)chemical potentials occurring in the disc are equal to the outer ones at the permeable boundaries (Fig. 1):

At $\Gamma_1 \cup \Gamma_2$, $\vec{u} = \vec{0}$, $\mu^\alpha = \overline{\mu^\alpha}$

At Γ_3, $\overline{\overline{\sigma}} \cdot \vec{n} = \vec{0}$, $\vec{\nabla}\mu^\alpha \cdot \vec{n} = 0$

At Γ_4, $\overline{\overline{\sigma}} \cdot \vec{n} = \vec{0}$, $\mu^\alpha = \overline{\mu^\alpha}$

At Γ_5, $\vec{u} \cdot \vec{e}_y = 0$, $(\overline{\overline{\sigma}} \cdot \vec{n}) \cdot \vec{e}_x = 0$, $\vec{\nabla}\mu^\alpha \cdot \vec{n} = 0$

where $\alpha = f, +, -$.

Nutrient exchange between IVD and plasma occurs via the annulus periphery and the inner part of the endplate:

At $\Gamma_1 \cup \Gamma_4$, $c^\omega = \overline{c^\omega}$

At $\Gamma_2 \cup \Gamma_3 \cup \Gamma_5$, $\vec{\nabla}c^\omega \cdot \vec{n} = 0$.

Γ_1 is reduced to the part of the endplate in contact with the nucleus in the degenerated reference disc: it becomes 10 mm smaller than in the healthy reference disc. The diffusion area is taken to be equal to the length of the permeable frontier.

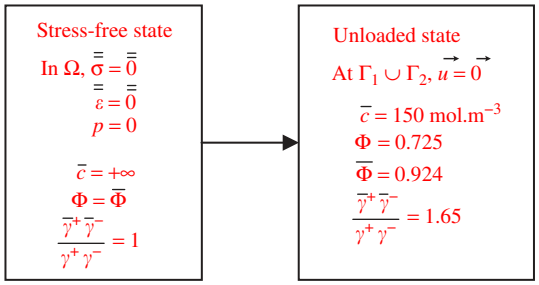

Fig. 2. Description of stress-free and unloaded states. Values of osmotic and activity coefficients are taken from Frijns et al. (1997) and Huyghe et al. (2003).

We take

$$J^f = -k(\rho_T^f \vec{\nabla}\mu^f + M^+ c^+ \vec{\nabla}\mu^+ + M^- c^- \vec{\nabla}\mu^-),$$

$$J^+ = c^+ J^f - \frac{D^+ M^+ \phi c^+}{RT}\vec{\nabla}\mu^+$$

and

$$J^- = c^- J^f - \frac{D^- M^- \phi c^-}{RT}\vec{\nabla}\mu^-$$

At the interface between two subdomains Ω_1 and Ω_2:

$$(\overline{\overline{\sigma}}_{\Omega_1} - \overline{\overline{\sigma}}_{\Omega_2}) \cdot \vec{n} = \vec{0}$$

$$(\overrightarrow{v^s_{\Omega_1}} - \overrightarrow{v^s_{\Omega_2}}) \cdot \vec{n} = 0$$

$$(J^f_{\Omega_1} - J^f_{\Omega_2}) \cdot \vec{n} = 0$$

$$(J^+_{\Omega_1} - J^+_{\Omega_2}) \cdot \vec{n} = 0$$

$$(J^-_{\Omega_1} - J^-_{\Omega_2}) \cdot \vec{n} = 0$$

$$((\phi D \vec{\nabla} c^\omega)_{\Omega_1} - (\phi D \vec{\nabla} c^\omega)_{\Omega_2}) \cdot \vec{n} = 0$$

2.4. Properties of healthy and degenerated discs

Some properties obtained in the literature (porosity, FCD and cell density) were based on measurements performed in the unloaded state, but not in the stress-free state. So they are directly assigned to disc equilibrium and their corresponding values in the stress-free state can be estimated recursively (Wilson et al., 2005).

Two property sets were assigned to healthy and degenerated discs. Assuming the occurrence of small perturbations (Sun et al., 1999; Yao and Gu, 2007), elastic mechanical properties required the elastic modulus E and Poisson's ratio v to be defined. Tables 1–4 summarize the osmomechanical properties, the constants, the cell density in the unloaded state and the properties of nutrients, respectively. The apparent diffusion coefficients in the tissue of small solutes such as oxygen, glucose and lactate $D_{tissue}{}^{\omega} = \phi D^{\omega}$ are linked to their diffusion coefficient in water $D_{water}{}^{\omega}$ by the following relation (Mackie and Meares, 1955):

$$D^{\omega}_{tissue} = \left(\frac{\phi}{2-\phi}\right)^2 D^{\omega}_{water} \tag{33}$$

The above two sets of properties were used as reference values in the parametric study to design healthy and degenerated IVDs. Elastic modulus, FCD, porosity, cell density and endplate diffusive area were varied individually up to 50% of the reference value to investigate their effects on the nutrient concentration profiles at equilibrium.

2.5. Numerical method of resolution

The finite element formulation was implemented in the COMSOL Multiphysics 3.3 software program. The Newton–Raphson method was used to solve the nonlinear equations. After determining the optimum mesh size, a mesh composed of 792 0.5 mm quadratic Lagrange quads in the healthy case (768 in the degenerated case) was selected.

3. Results

The present model predicted the relationships between nutrient concentration profiles and the properties of healthy and degenerated discs in the unloaded state.

The critical concentrations were the minimum glucose and oxygen concentrations and the maximum lactate concentration. These values occurred in the middle of the disc, near the interface between the inner and the outer anterior annulus in both healthy cases and at the top of the endplate in the degenerated case (Fig. 3).

At the mid-horizontal plane, the oxygen pressure and glucose concentration decrease from outer to inner annulus and increase towards the nucleus, while the lactate concentration shows the opposite tendency. Since the diffusion distance has been increased in the anterior part and decreased in the posterior part, the concentration asymmetry between the two parts is more marked in the non-uniform configuration than in the uniform configuration (Fig. 4a). The oxygen pressure and lactate concentration are in the range of human physiological values measured by Bartels et al. (1998) (Fig. 4b and c).

Fig. 5 shows the critical nutrient concentrations (or concentration peaks) normalized with respect to the reference values,

Table 1
Disc osmomechanical properties in the unloaded state, taken to be homogeneous in each subdomain.

	Nucleus pulposus	Anterior inner annulus	Posterior inner annulus	Anterior outer annulus	Posterior outer annulus	Endplate	References
Healthy disc							
Elastic modulus (MPa)	0.2	1.0	1.0	1.0	1.0	25.0	Best et al. (1994),
Poisson's ratio	0.1	0.1	0.1	0.1	0.1	0.1	Cheung et al. (2003),
Permeability ($m^4 N^{-1} s^{-1}$)	9.0×10^{-16}	2.5E−16	2.5E−16	2.5E−16	2.5E−16	7.0E−15	Drost et al. (1995), Frijns et al. (1997), Huyghe et al. (2003), Iatridis et al. (1998), Johannessen and Elliott (2005), Whyne et al. (2001)
Porosity	0.850	0.835	0.825	0.785	0.740	0.710	Antoniou et al. (1996),
FCD ($mol\,m^{-3}$)	350	340	290	250	200	195	Antoniou et al. (2001), Urban et al. (1979)
Degenerated disc							
Elastic modulus (MPa)	1.0	1.0	1.0	1.0	1.0	25.0	Best et al. (1994),
Poisson's ratio	0.1	0.1	0.1	0.1	0.1	0.1	Cheung et al. (2003),
Permeability ($m^4 N^{-1} s^{-1}$)	2.5E−16	2.5E−16	2.5E−16	2.5E−16	2.5E−16	7.0E−15	Drost et al. (1995), Frijns et al. (1997), Huyghe et al. (2003), Iatridis et al. (1998), Johannessen and Elliott (2005), Whyne et al. (2001)
Porosity	0.775	0.760	0.760	0.720	0.720	0.655	Antoniou et al. (1996),
FCD ($mol\,m^{-3}$)	220	230	230	150	150	189	Antoniou et al. (2001), Urban et al. (1979)

Table 2
Constants.

Diffusion coefficient of the cation D^+	$5.0 \times 10^{-10}\,m^2\,s^{-1}$	Frijns et al. (1997), Maroudas (1988), Sun et al. (1999)
Diffusion coefficient of the anion D^-	$8.0 \times 10^{-10}\,m^2\,s^{-1}$	
Universal gas constant R	$8.314472\,J\,mol^{-1}\,K^{-1}$	–
Absolute temperature T	310 K	–
Faraday constant F	$96{,}500\,C\,mol^{-1}$	–
Unitary concentration c_0	$1\,mol\,m^{-3}$	–
Solubility of oxygen in water s	$1.0268 \times 10^{-2}\,nmol\,kPa^{-1}\,mm^{-3}$	O'Hare et al. (1991)

Table 3
Cell density in the unloaded state, taken to be homogeneous in each subdomain. Data from Maroudas et al. (1975), corrected by a living cell rate of 90% in the case of a healthy disc (Bibby et al., 2002) and 40% in the case of a degenerated disc (Gruber and Hanley, 1998).

	Cell density (in $10^3\,cell\,mm^{-3}$)		Living cell density (in $10^3\,cell\,mm^{-3}$)	
	Healthy disc	Degenerated disc	Healthy disc	Degenerated disc
Endplate	15.0	17.0	13.5	6.8
Outer annulus	8.0	12.0	7.2	4.8
Inner annulus	6.0	8.0	5.4	3.2
Nucleus	4.0	5.0	3.6	2.0

Table 4
Properties involving nutrients.

		Oxygen	Lactate	Glucose
Diffusion coefficient in water		$10.8\,mm^2\,h^{-1}$[a]	$5.0\,mm^2\,h^{-1}$[b]	$3.3\,mm^2\,h^{-1}$[c]
Boundary conditions	Plasma (c^{plasma})	9.5 kPa[b]	$1.0\,mol\,m^{-3}$[b]	$5.6\,mol\,m^{-3}$[d]
	Annulus	9.5 kPa[b]	$1.0\,mol\,m^{-3}$[e]	$5.6\,mol\,m^{-3}$
	Endplate	7.6 kPa	$0.35\,mol\,m^{-3}$[b]	$3.92\,mol\,m^{-3}$[d]

For boundary conditions where no data are available in the literature, $\bar{c} = 0.8c^{plasma}$ at endplate frontier and $\bar{c} = c^{plasma}$ at annulus frontier (Sélard et al., 2003).
[a] Wilke and Chang (1955).
[b] Holm et al. (1981).
[c] Boubriak et al. (2006).
[d] Maroudas et al. (1975).
[e] Bartels et al. (1998).

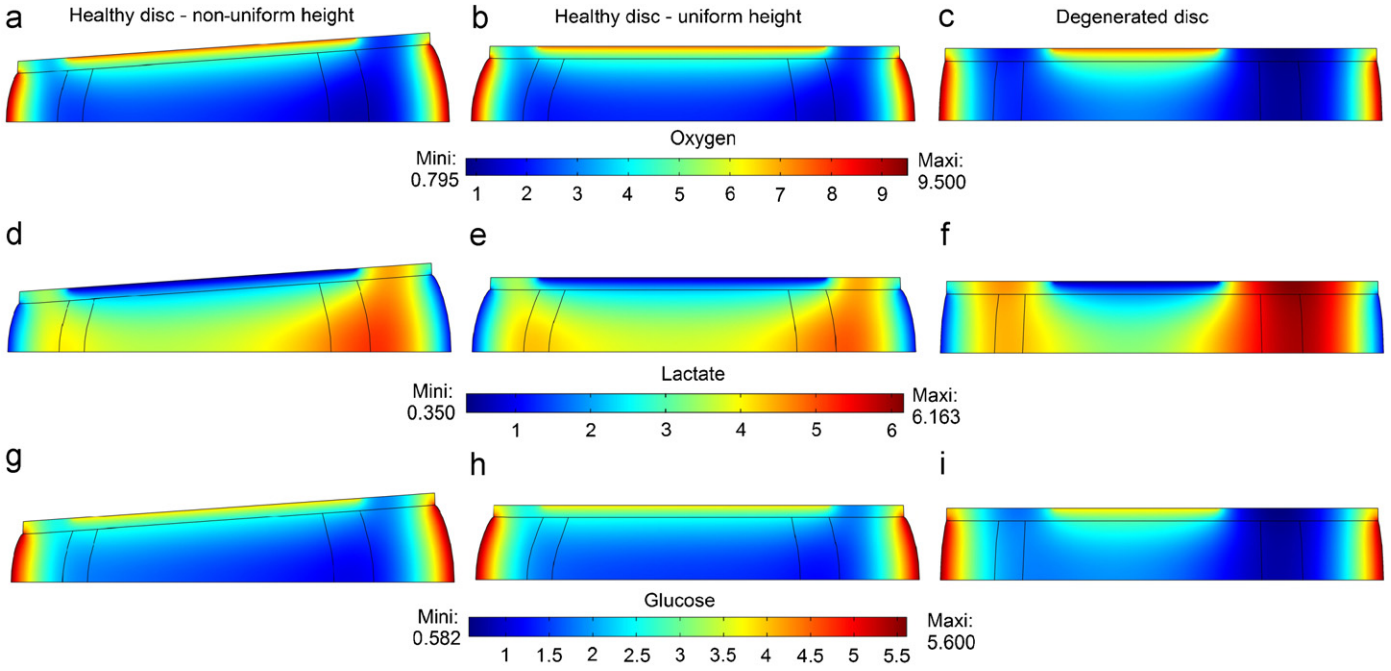

Fig. 3. Oxygen pressure (kPa) (a–c) and lactate (d–f) and glucose (g–i) concentrations ($nmol\,mm^{-3}$) in the healthy disc with non-uniform height (a, d, g), in the healthy disc with uniform height (b, e, h) and in the degenerated disc (c, f, i).

versus disc properties. The data for the healthy disc with non-uniform height were not shown, because their trends are the same as those for the healthy disc with uniform height.

In the healthy disc, an increase in the elastic modulus or a decrease in the FCD leads to an increase in the oxygen and glucose concentration peaks and to a decrease in the lactate peak. A 50% change in either parameter results in a maximum change of 4%, 8% and 7% in the lactate, oxygen and glucose peaks, respectively (Fig. 5a and e). In the degenerated disc, the range of oxygen and lactate concentration changes is less than 5%, whereas that of the glucose concentration amounts to 13% (Fig. 5b and f).

In the healthy disc, a 16% decrease in the porosity suffices to abolish glucose from the critical zones of the disc (Fig. 5c). A 50% increase in cell density or a 26% decrease in endplate diffusion area leads to a critical glucose concentration of less than 0.4 nmol mm^{-3} (Fig. 5g and i), a threshold below which the cells begin to die (Bibby et al., 2005); whereas, the glucose concentration peak increases by about 50% when the cell density decreases by 30%. Boundary conditions also affect the other solutes: a 30% increase in the endplate diffusion area leads to a 10% and 23% increase in the glucose and oxygen peaks, respectively, and an 11% decrease in the lactate peak.

Opposite changes always occur between the glucose and oxygen concentrations and the lactate concentration. In the degenerated disc, the magnitude and direction of the changes in the nutrient concentrations are similar to those observed in the healthy disc, except for glucose, which shows significantly larger changes (Fig. 5b, d, f, h and j). For instance, a 26% increase in cell density results in the disappearance of glucose from the critical areas of the degenerated disc, whereas the glucose peak remains at 62% of the reference value in the healthy disc.

It emerges that the elastic modulus and FCD have weaker effects on the nutrient concentration peaks than the porosity, cell density and endplate boundary conditions.

4. Discussion

The present IVD model, in which osmomechanical behavior is coupled to nutrient diffusion processes, is used to investigate the sensitivity of nutrient spatial distribution to changes in the osmomechanical and metabolic properties of healthy and degenerated discs.

Elastic modulus and FCD control lateral disc deformation according to the boundary conditions and consequently the diffusion distance from the annulus periphery to the nucleus. They have weak effects because the distances vary slightly and the diffusion from the annulus contributes less to cellular metabolism than that from the endplate. On the contrary, porosity, cell density and endplate diffusion area contribute importantly to maintaining discal homeostasis: even quite small changes in these parameters can lead to the complete disappearance of glucose from some critical regions of the disc. Since diffusion coefficients are linked to porosity (see Eq. (33)), the nutrient concentration profiles depend on diffusion distances and coefficients in the IVD, cell metabolic reaction rate and endplate boundary conditions. The critical zones in the disc are those showing the highest proteoglycan losses, i.e., between 30% and 40% in the nucleus and inner annulus (Table 1). Insufficient cell nutrient supplies may therefore promote degeneration (Bibby and Urban, 2004).

The nucleus pressure in the healthy disc with uniform height (0.26 MPa) is close to the nucleus pressure measured by Wilke et al. (1999) after 7 h of rest (0.24 MPa) and is higher than the nucleus pressure in the degenerated disc (0.12 MPa), as found by Nachemson (1960). Most of the oxygen pressure and lactate concentration peaks measured *in vitro* by Bartels et al. (1998)

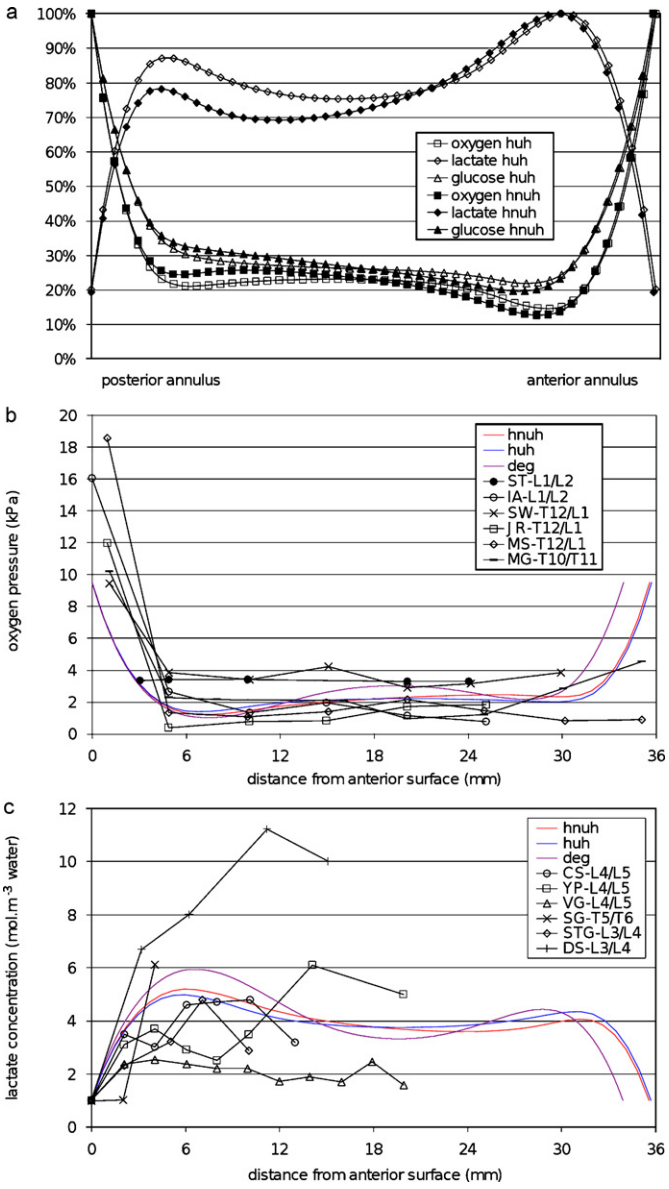

Fig. 4. Nutrient concentrations at the interface between sagittal and mid-horizontal planes (a) Normalized concentrations of oxygen, lactate and glucose in the healthy discs. Comparison between numerical results obtained by the present model and experimental data issued from Bartels et al. (1998) in terms of (b) oxygen pressure, (c) lactate concentration. huh: healthy disc with uniform height, hnuh: healthy disc with non-uniform height, deg: degenerated disc, XX-L4/L5: patient designation duplicated from the article of Bartels et al. (1998) followed by the level of the IVD where profiles were measured.

(0.67–4 kPa and 2–6 nmol mm^{-3}, respectively) were in line with the modeling values obtained here for the healthy disc with uniform height (1.4 kPa and 5.0 nmol mm^{-3}, respectively) and for the degenerated disc (1.0 kPa and 5.9 nmol mm^{-3}, respectively) (Fig. 3b, c, e and f). Moreover, the computed oxygen pressure profiles were in agreement with the experimental ones, which generally showed a decrease from outer to inner annulus and a slight increase towards the nucleus (Fig. 4b and c). Opposite changes occurred between the lactate and oxygen profiles, as observed experimentally.

Elsewhere, the model predicts higher lactate levels, and thus lower pH levels (see Eq. (28)), in the degenerated disc than in the healthy disc (Fig. 3e and f), in agreement with experimental data (Kitano et al., 1993). As the disc degenerates, the porosity and

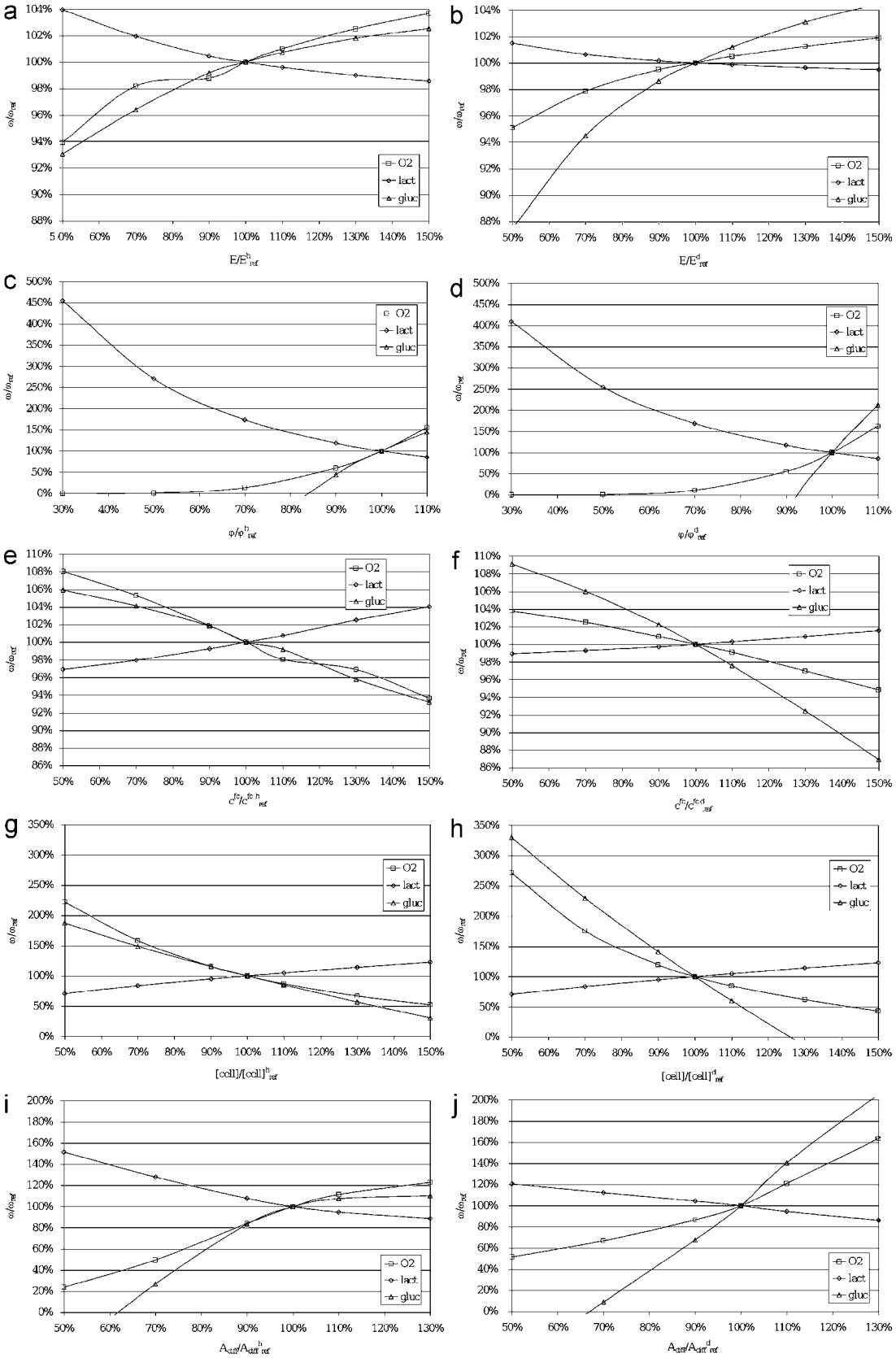

Fig. 5. Normalized changes in nutrient concentration peaks ω versus properties: (a) and (b) elastic modulus, (c) and (d) porosity, (e) and (f) FCD, (g) and (h) cell density, (i) and (j) endplate diffusion area) in the healthy with uniform height (left) and in the degenerated disc (right). X_{ref} is the reference value.

endplate diffusion area decrease, obstructing lactate evacuation. The changes in these two parameters occurring during degeneration greatly override changes in other parameters, such as the stiffness increase and the loss of proteoglycan and living cells, which have the opposite effects on lactate. Low pH are problematic because they reduce cell viability (Bibby and Urban, 2004) and slow the renewal of the extracellular matrix (Ohshima and Urban, 1992).

This study has some limitations. Comparisons between the numerical and physiological values were difficult because few experimental data are available and there exist strong variations between individuals. The 2-D formulation is rather restrictive: a 3-D formulation would give more realistic geometry and make comparisons possible between solute concentrations in sagittal versus frontal planes. Moreover, the 2-D plane strain hypothesis leads to an overestimation of the lateral displacement compared to a 3-D model, which would be similarly loaded. No distinction was made between intra- and extrafibrillar fluid and thus their exchange was not taken into account (Huyghe et al., 2003; Schroeder et al., 2007). The model could be enhanced using a more complex approach applicable to large deformations, distinguishing between hyperelastic extracellular matrix and viscoelastic collagen fibers (Schroeder et al., 2006). It could also be easily extended to the study of the transient behavior of the disc, adding temporal terms to the mass conservation equations.

This model combining disc osmomechanical behavior and nutrient diffusion processes provides a tool for investigating time-evolving nutrient concentration profiles in a loaded disc. Our next step might focus on the effects of diurnal loading on cellular metabolism. Given the effects of glucose and pH on cell viability and metabolism, this model could be further improved by referring the time-related changes in the numbers of living cells and metabolic rate to the nutrient concentrations and pH in the disc, to predict lifelong proteoglycan concentration changes. This coupled model opens new perspectives for investigating IVD degeneration mechanisms.

Conflict of interest

None.

References

Antoniou, J., Steffen, T., Nelson, F., Winterbottom, N., Hollander, A.P., Poole, R.A., Aebi, M., Alini, M., 1996. The human lumbar intervertebral disc: evidence for changes in the biosynthesis and denaturation of the extracellular matrix with growth, maturation, ageing, and degeneration. Journal of Clinical Investigation 98, 996–1003.

Antoniou, J., Arlet, V., Goswami, T., Aebi, M., Alini, M., 2001. Elevated synthetic activity in the convex side of scoliotic intervertebral discs and endplates compared with normal tissues. Spine 26, E198–E206.

Bartels, E.M., Fairbank, J.C., Winlove, C.P., Urban, J.P., 1998. Oxygen and lactate concentrations measured in vivo in the intervertebral discs of patients with scoliosis and back pain. Spine 23, 1–8.

Best, B.A., Guilak, F., Setton, L.A., Zhu, W., Saed-Nejad, F., Ratcliffe, A., Weidenbaum, M., Mow, V.C., 1994. Compressive mechanical properties of the human anulus fibrosus and their relationship to biochemical composition. Spine 19, 212–221.

Bibby, S.R.S., Urban, J.P.G., 2004. Effect of nutrient deprivation on the viability of intervertebral disc cells. European Spine Journal 13, 695–701.

Bibby, S.R.S., Fairbank, J.C.T., Urban, M.R., Urban, J.P.G., 2002. Cell viability in scoliotic discs in relation to disc deformity and nutrient levels. Spine 27, 2220–2228.

Bibby, S.R.S., Jones, D.A., Ripley, R.M., Urban, J.P.G., 2005. Metabolism of the intervertebral disc: effects of low levels of oxygen, glucose, and pH on rates of energy metabolism of bovine nucleus pulposus cells. Spine 30, 487–496.

Boos, N., Wallin, A., Gbedegbegnon, T., Aebi, M., Boesch, C., 1993. Quantitative MR imaging of lumbar intervertebral disks and vertebral bodies: influence of diurnal water content variations. Radiology 188, 351–354.

Boubriak, O.A., Urban, J.P.G., Cui, Z., 2006. Monitoring of metabolite gradients in tissue-engineered constructs. Journal of the Royal Society 3, 637–648.

Brodin, H., 1955. Paths of nutrition in articular cartilage and intervertebral discs. Acta Orthopaedica Scandinavica 24, 177–183.

Cheung, J.T., Zhang, M., Chow, D.H., 2003. Biomechanical responses of the intervertebral joints to static and vibrational loading: a finite element study. Clinical Biomechanics 18, 790–799.

Drost, M.R., Willems, P., Snijders, H., Huyghe, J.M., Janssen, J.D., Huson, A., 1995. Confined compression of canine annulus fibrosus under chemical and mechanical loading. Journal of Biomechanical Engineering 117, 390–396.

Frijns, A.J.H., Huyghe, J.M., Janssen, J.D., 1997. A validation of the quadriphasic mixture theory for intervertebral disc tissue. International Journal of Engineering Science 35, 1419–1429.

Gruber, H.E., Hanley, E.N.J., 1998. Analysis of aging and degeneration of the human intervertebral disc. Comparison of surgical specimens with normal controls. Spine 23, 751–757.

Holm, S., Maroudas, A., Urban, J.P., Selstam, G., Nachemson, A., 1981. Nutrition of the intervertebral disc: solute transport and metabolism. Connective Tissue Research 8, 101–119.

Huang, C., Gu, W.Y., 2008. Effects of mechanical compression on metabolism and distribution of oxygen and lactate in intervertebral disc. Journal of Biomechanics 41, 1184–1196.

Huyghe, J.M., Janssen, J.D., 1997. Quadriphasic mechanics of swelling incompressible porous media. International Journal of Engineering Science 35, 793–802.

Huyghe, J.M., Houben, G.B., Drost, M.R., van Donkelaar, C.C., 2003. An ionised/non-ionised dual porosity model of intervertebral disc tissue. Biomechanics and Modeling in Mechanobiology 2, 3–19.

Iatridis, J.C., Setton, L.A., Foster, R.J., Rawlins, B.A., Weidenbaum, M., Mow, V.C., 1998. Degeneration affects the anisotropic and nonlinear behaviors of human anulus fibrosus in compression. Journal of Biomechanics 31, 535–544.

Johannessen, W., Elliott, D.M., 2005. Effects of degeneration on the biphasic material properties of human nucleus pulposus in confined compression. Spine 30, E724–E729.

Katz, M.M., Hargens, A.R., Garfin, S.R., 1986. Intervertebral disc nutrition. Diffusion versus convection. Clinical Orthopaedics and Related Research 210, 243–245.

Kimura, S., Steinbach, G.C., Watenpaugh, D.E., Hargens, A.R., 2001. Lumbar spine disc height and curvature responses to an axial load generated by a compression device compatible with magnetic resonance imaging. Spine 26, 2596–2600.

Kitano, T., Zerwekh, J.E., Usui, Y., Edwards, M.L., Flicker, P.L., Mooney, V., 1993. Biochemical changes associated with the symptomatic human intervertebral disk. Clinical Orthopaedics and Related Research 293, 372–377.

Lavaste, F., Skalli, W., Robin, S., Roy-Camille, R., Mazel, C., 1992. Three-dimensional geometrical and mechanical modelling of the lumbar spine. Journal of Biomechanics 25, 1153–1164.

Loret, B., Simões, F.M.S., 2004. Articular cartilage with intra- and extrafibrillar waters: a chemo-mechanical model. Mechanics of Materials 36, 515–541.

Mackie, J., Meares, P., 1955. The diffusion of electrolytes in a cation-exchange resin membrane. Proceedings of the Royal Society of London. Series A, Mathematical and Physical Sciences 232, 498–518.

Maroudas, A., 1988. Nutrition and metabolism of the intervertebral disc. In: Ghosh, P. (Ed.), The Biology of the Intervertebral Disc. CRC Press, Boca Raton, FL, pp. 1–37.

Maroudas, A., Stockwell, R.A., Nachemson, A., Urban, J., 1975. Factors involved in the nutrition of the human lumbar intervertebral disc: cellularity and diffusion of glucose in vitro. Journal of Anatomy 120, 113–130.

Nachemson, A., 1960. Lumbar intradiscal pressure. Experimental studies on post-mortem material. Acta Orthopaedica Scandinavica 43 (Supplementum), 1–104.

O'Hare, D., Winlove, C.P., Parker, K.H., 1991. Electrochemical method for direct measurement of oxygen concentration and diffusivity in the intervertebral disc: electrochemical characterization and tissue–sensor interactions. Journal of Biomedical Engineering 13, 304–312.

Ohshima, H., Urban, J.P., 1992. The effect of lactate and pH on proteoglycan and protein synthesis rates in the intervertebral disc. Spine 17, 1079–1082.

Schroeder, Y., Wilson, W., Huyghe, J.M., Baaijens, F.P.T., 2006. Osmoviscoelastic finite element model of the intervertebral disc. European Spine Journal 15 (Suppl. 3), S361–S371.

Schroeder, Y., Sivan, S., Wilson, W., Merkher, Y., Huyghe, J.M., Maroudas, A., Baaijens, F.P.T., 2007. Are disc pressure, stress and osmolarity affected by intra- and extrafibrillar fluid exchange? Journal of Orthopaedic Research 25, 1317–1324.

Sélard, E., Shirazi-Adl, A., Urban, J.P.G., 2003. Finite element study of nutrient diffusion in the human intervertebral disc. Spine 28, 1945–1953.

Soukane, D.M., Shirazi-Adl, A., Urban, J.P.G., 2005. Analysis of nonlinear coupled diffusion of oxygen and lactic acid in intervertebral discs. Journal of Biomechanical Engineering 127, 1121–1126.

Soukane, D.M., Shirazi-Adl, A., Urban, J.P.G., 2007. Computation of coupled diffusion of oxygen, glucose and lactic acid in an intervertebral disc. Journal of Biomechanics 40, 2645–2654.

Sun, D.N., Gu, W.Y., Guo, X.E., Lai, W.M., Mow, V.C., 1999. A mixed finite element formulation of triphasic mechano-electrochemical theory for charged, hydrated biological soft tissues. International Journal for Numerical Methods in Engineering 45, 1375–1402.

Thompson, J.P., Pearce, R.H., Schechter, M.T., Adams, M.E., Tsang, I.K., Bishop, P.B., 1990. Preliminary evaluation of a scheme for grading the gross morphology of the human intervertebral disc. Spine 15, 411–415.

Urban, J.P., McMullin, J.F., 1985. Swelling pressure of the inervertebral disc: influence of proteoglycan and collagen contents. Biorheology 22, 145–157.
Urban, J.P., Maroudas, A., Bayliss, M.T., Dillon, J., 1979. Swelling pressures of proteoglycans at the concentrations found in cartilaginous tissues. Biorheology 16, 447–464.
Urban, J.P.G., Holm, S., Maroudas, A., Nachemson, A., 1982. Nutrition of the intervertebral disc: effect of fluid flow on solute transport. Clinical Orthopaedics and Related Research 170, 296–302.
Whyne, C.M., Hu, S.S., Lotz, J.C., 2001. Parametric finite element analysis of vertebral bodies affected by tumors. Journal of Biomechanics 34, 1317–1324.
Wilke, C.R., Chang, P., 1955. Correlation of diffusion coefficients in dilute solutions. American Institute of Chemical Engineers Journal 1, 264–270.
Wilke, H.J., Neef, P., Caimi, M., Hoogland, T., Claes, L.E., 1999. New in vivo measurements of pressures in the intervertebral disc in daily life. Spine 24, 755–762.
Wilson, W., van Donkelaar, C.C., van Rietbergen, B., Huiskes, R., 2005. A fibril-reinforced poroviscoelastic swelling model for articular cartilage. Journal of Biomechanics 38, 1195–1204.
Yao, H., Gu, W.Y., 2007. Three-dimensional inhomogeneous triphasic finite-element analysis of physical signals and solute transport in human intervertebral disc under axial compression. Journal of Biomechanics 40, 2071–2077.